Open Access

Advances in Environmental and Engineering Research

LIDSEN Publishing Inc.

Original Research

Kinetics and Thermodynamics of the Pyrolysis of Waste Polystyrene over Natural Clay

Ghulam Ali *, Jan Nisar

National Centre of Excellence in Physical Chemistry, University of Peshawar, 25120, Peshawar, Pakistan; E-Mails: ghulamali@uop.edu.pk; jan_nisar@uop.edu.pk

***Correspondence:** Ghulam Ali; E-Mail: ghulamali@uop.edu.pk

Academic Editor: Amanda Laca

Adv Environ Eng Res
2022, volume 3, issue 4
doi:10.21926/aeer.2204044

Received: July 22, 2022
Accepted: October 23, 2022
Published: November 01, 2022

Abstract

Due to the massive increase in polymer manufacture, there has been a remarkable increase in plastic waste. With fewer landfills being used to dump plastic waste each year, it is becoming increasingly important to use effective recycling methods for plastic waste decomposition. In the present work, waste polystyrene was degraded in the presence of natural clay ($K_{0.02}$, $Ca_{0.15}$ [$Mg_{0.25}$, $Al_{0.69}$, $Fe_{0.06}$], [$Si_{2.0}$, $Al_{0.6}$] $O_{6.8}$ (O_{10}) nH_2O). The waste polymer was pyrolyzed at different heating rates i.e., 5, 10, 15 and 20°C min^{-1} in an inert environment using nitrogen within the temperature range of 40 to 600°C. Thermogravimetric data were interpreted using various models, including fitting kinetic methods i.e., Coats-Redfern and model-free methods i.e., Ozawa-Flynn-Wall, Kissinger-Akahira-Sunose and Friedman method. The activation energy determined by Coats-Redfern, Ozawa-Flynn-Wall, Kissinger-Akahira-Sunose and Friedman models were in the range of 83.22-150.37, 74.52-133.71, 73.16-131.23, and 78.40-140.67 $kJmol^{-1}$, respectively. Among them, the lowest activation energy for polystyrene degradation was observed using Kissinger-Akahira-Sunose method. The calculated kinetic parameters would be useful in determining the reaction mechanism of the solid-state reactions in a real system.

Keywords

Waste polystyrene; pyrolysis; thermogravimetry; kinetic models; activation energy

1. Introduction

Polystyrene (PS) is a tough, low-cost plastic that is used in a wide range of applications in our daily life, such as kitchen appliances, toys, customer goods, food protective packaging, computers and hairdryer, etc. However, due to their non-biodegradable nature, the disposal of these solid wastes causes serious environmental problems. Waste polystyrene (WPS) accounts for about 10 wt.% of total plastic waste [1-3]. Numerous techniques have been used to recycle WPS, the most commonly used are physical recycling by blending and mixing and chemical recycling [4, 5]. Another common technique used to dispose of plastic waste is thermal decomposition. Recycling of WPS by thermal incineration collects many useful products and therefore plays an important role in solving waste disposal problems [6].

For the decomposition of waste polymer into useful products through the pyrolysis process, it is important to understand the background knowledge of reaction pathways and pyrolysis mechanism. If the results of a complete mechanical model in relations of pyrolysis mechanism and overall rates can be thoroughly calculated as the kinetic rate parameters, then the reaction pathways to specific products can be examined [7, 8]. Therefore, the focus of the present work was to study the thermal degradation of waste PS at low temperatures and to determine the kinetic parameters using model fitting i.e., Coats-Redfern (CR), and model-free methods i.e., Ozawa-Flynn-Wall (OFW), Kissinger-Akahira-Sunose (KAS), and Friedman (FM). The most appropriate kinetic model along with their thermodynamic parameters was determined by the pyrolysis process.

Model-fitting techniques were commonly used for studying kinetics of solid-state reactions due to their capability to directly calculate activation energy (Ea) and frequency factor (A) from individual thermogravimetric analyzer data. However, these techniques are affected by several problems and one among them is their incapability to uniquely calculate the reaction model, particularly for non-isothermal data. Though these models can be found to be statistically equivalent, the fitted kinetic parameters can fluctuate by an order of magnitude and therefore, the choice of a proper model can be problematic. Application of model-fitting techniques to non-isothermal data can result in greater values for kinetic parameters. On other hand, the model-free method is based on its straightforwardness and the anticipation of errors associated with the choice of a kinetic model [9-11]. Current studies have widely focused on the degradation of WPS for the production of fuel-like substances, however, there is still a lack of exploration of the kinetics of degradation [12, 13].

Şenocak et al. [14] investigated the thermal decomposition of WPS using a TGA, and the thermogravimetric data collected from TGA was further applied to the OFW equation to determine the kinetic parameters. The calculated activation energy for different fractions was in the range of 179.74 to 200.36 $kJmol^{-1}$ with first-order kinetics. Aboulkas and Nadifiyine [15] determined the activation energy of PS using the OFW method at a wide range of temperatures i.e., 600 to 900℃, and found an activation energy of 169 $kJmol^{-1}$. Singh and Singh [16] carried out the kinetics analysis of the decomposition of PS. Several catalysts were utilized to study the kinetic parameters of PS at 400℃ and the values of activation energy at different heating rates were 359, 360, 361 and 361 $kJmol^{-1}$.

Oh et al. [17] evaluated the thermal decomposition of PS at different heating rates in supercritical acetone and inert conditions. The thermogravimetric data was interpreted using Arrhenius equation and kinetic parameters determined in supercritical acetone were compared with nitrogen atmosphere. The results showed that the average activation energy calculated in supercritical acetone medium ranged from 167.0 to 195.8 $kJmol^{-1}$, while in the nitrogen atmosphere it ranged from 245.4 to 251.5 $kJmol^{-1}$. Kyaw et al. [18] studied the pyrolysis of PS in the temperature range of 370 to 420°C and observed that the selectivity for styrene trimers, dimers and monomers decreased as the reaction proceeded, due to the difficulty in the decomposition of benzene rings phenyl radicals. The degradation was formulated to be first-order kinetics with activation energy equal to 157 $kJmol^{-1}$. Peterson [19] carried out the thermal and thermo-oxidative decomposition of WPS through thermogravimetry. The thermogravimetric data was interpreted for the determination of kinetic parameters. Under inert conditions, the activation energy was 200 $kJmol^{-1}$.

According to the recommendations made by the Kinetics Committee of the International Confederation for Thermal Analysis and Calorimetry [20, 21], consistent kinetics parameters could be gained if the sample is exposed to the pyrolysis process at not less than three different heating rates in an appropriately standardized instrument. Therefore, considering this recommendation, the present study was performed at four different heating rates of 5, 10, 15 and 20°C/min on an appropriately calibrated instrument and the kinetics parameters were determined using CR, OFW, KAS and FM models. Thermodynamic parameters of WPS decomposition reaction would be very helpful for the optimization of reaction engineering in industrial processes. Moreover, the kinetics and thermodynamic parameters would be very useful in determining the solid-state reaction mechanisms in a real system.

2. Experimental

2.1 Material

WPS was collected from a recycling site in a local shopping mall and shredded into small pieces with a size of 50-70 mesh by a shredder. Clay was collected from a clay rock. WPS and catalyst were mixed in the ratio of 97:3 and stored in a desiccator for further studies.

2.2 Thermogravimetric Analysis

Thermogravimetric analysis of WPS and clay mixture was carried out in a Simultaneous Thermogravimetric analyzer (Perkin-Elmer). Approximately 7 mg of each sample was taken in an alumina pan and heated at four different heating rates, i.e. 5, 10, 15 and 20°C/min, from 40°C to a final temperature of 600 °C. After complete weight loss, the data was collected and the kinetics parameters were calculated by CR, OFW, KAS and FM kinetic models.

2.3 Kinetics Analysis

Most of the solid-state degradation reaction follows Equation 1:

$$A_{solid} \leftrightarrow B_{solid} + C_{gas} \quad (1)$$

The rate can be investigated from the product in the form of three major variables: the pressure P, the temperature T, and the degree of conversion α [20, 22], as shown in Equation 2.

$$\frac{d\alpha}{dt} = k(T)\, f(\alpha)h(P) \tag{2}$$

where t is time and the pressure dependence, *h(P)* is neglected in most kinetic models used in thermal degradation. When the products or reactants are gases then the pressure may have a major effect on the kinetics of processes. The term *h(P)* is considered to be constant throughout the experiments. Therefore, most kinetic models used in the field of thermal analysis consider the rate as a function of only two variables, α and T, in such case the above equation becomes Equation 3:

$$\frac{d\alpha}{dt} = k(T)f(\alpha) \tag{3}$$

In Equation 3, *k(T)* is the rate constant and $f(\alpha)$ is the fraction of conversion. Equation 3 explains the rate of single-step reaction, however, the physical properties calculated by the pyrolysis methods are not reactants specific i.e. cannot be linked directly to particular reactions of molecules. Therefore, the value of α particularly reflects the development of the reactant to product conversion in all the cracking processes. The complete transformation commonly involves many reactions, in other words, each with its specific degree of conversion. The entire transformation process of the two parallel reactions can be explained by Equation 4 [20, 23].

$$\frac{d\alpha}{dt} = k_1(T)f(\alpha_1) + \frac{d\alpha}{dt} = k_2(T)f(\alpha_2) \tag{4}$$

where α_1 and α_2 are the degree of conversion associated with two individual reactions, and their sum is the total conversion rate as shown in Equation 5:

$$\alpha = \alpha_1 + \alpha_2 \tag{5}$$

However, if a process is found to follow a one-step equation, we should not determine that the mechanism of the reaction involves one single step. Generally, a mechanism involves many steps, one of which determines the overall rate of the reaction. This happens in the mechanism of two consecutive reactions when the first reaction is slower than the second. Then, the first reaction would determine the overall rate of reaction, which would obey a single step, although the mechanism involves two steps.

The dependence of the reaction rate of a process on temperature is elaborated by Arrhenius equation, as shown in Equation 6:

$$k(T) = Ae^{-Ea/RT} \tag{6}$$

where *R, Ea* and *A* are universal gas constant, activation energy and pre-exponential factor, respectively. Normally, the actual kinetic parameters are functions of the intrinsic parameters of the separate steps. Hence, the kinetics of solid-state reaction can be explained by Equation 7:

$$\frac{d\alpha}{dt} = Ae^{-Ea/RT}f(\alpha) \tag{7}$$

where the temperature of the sample varies with time, so the rate of reaction is shown in Equation 8:

$$\beta = \frac{dT}{dt} \tag{8}$$

where β is the rate constant.

By combining and rearranging equations 7 and 8, the following Equation 9 is obtained:

$$\frac{d\alpha}{dT} = \frac{A}{\beta} e^{-Ea/RT} f(\alpha) \tag{9}$$

By separating the variables and then integrating and rearranging Equation 9, Equation 10 was derived [24]:

$$g(\alpha) = \int_{\alpha_0}^{\alpha} \frac{d\alpha}{\int(\alpha)} = \frac{A}{\beta} \int_{T_0}^{T} e^{-Ea/RT} \tag{10}$$

Equation 10 is the foundation for a variety of integral methods. Various approximate solutions have been proposed, leading to a variety of integral methods.

When *x* is equal to *Ea/RT*, the following Equation 11 is obtained:

$$\int_{T_0}^{T} e^{-Ea/RT}\, dT = -\frac{Ea}{R} \int_{x_0}^{x} \frac{e^{-x}}{x^2} dx \tag{11}$$

Let the right-hand side of Equation 11 be equal to *p(x)*, Equation 12 is obtained:

$$p(x) = -\frac{Ea}{R} \int_{x_0}^{x} \frac{e^{-x}}{x^2} dx \tag{12}$$

By using integration by parts, Equation 12 leads to Equation 13:

$$p(x) = \frac{Ea}{R} \frac{e^{-x}}{x} l^{x}{}_{0} + \frac{Ea}{R} \int_{x_0}^{x} \frac{e^{-x}}{x} dx = \frac{Ea}{R} \left[\frac{e^{-x}}{x} - \int_{x}^{\infty} \frac{e^{-x}}{x} dx \right] - \frac{Ea}{R} \left[\frac{e^{-x_0}}{x_0} - \int_{x}^{\infty} \frac{e^{-x}}{x} dx \right] \tag{13}$$

The second term in Equation 13 can be neglected except that the values of *p(x)* becomes progressively smaller, so Equation 14 is obtained [25, 26].

$$p(x) = \frac{Ea}{R} \left[\frac{e^{-x}}{x} - \int_{x}^{\infty} \frac{e^{-x}}{x} dx \right] \tag{14}$$

The molecular structure, nuclear structure and flow of heat evaluated by exponential integral are almost equal to the asymptotic equation 15:

$$\int_{x}^{\infty} \frac{e^{-x}}{x} dx \cong e^{-x} \left(\frac{1}{x} - \frac{1!}{x^2} + \cdots + \left(-1 \right)^{n-1} \frac{(n-1)!}{x^n} + \cdots \right) \tag{15}$$

As the *p(x)* is equal to Equation 16:

$$p(x) = (-1)^n \frac{(n-1)!}{x^n} e^x \tag{16}$$

As the *g(α)* can be expressed as Equation 17:

$$g(\alpha) = \frac{AEa}{\beta R} p(x) \tag{17}$$

Taking the natural log and rearranging Equation 17, we obtain Equation 18:

$$ln\beta = ln\frac{AEa}{\beta R} + \ln p(x) \tag{18}$$

where Equation 18 is integrated with Doyle's approximation, i.e. when x ≥ 20, the function *p(x*) can be expressed as Equation 19 [27, 28]:

$$p(x) = 0.0048e^{-1.0516} \tag{19}$$

$$\ln p(x) = -2.315 + 0.4567x \tag{20}$$

The equation for *p(x)* is derived by numerical integration using the trapezoidal rule [29]. Substituting Equation 20 into Equation 18 obtained Equation 21:

$$\ln(\beta) = \ln\left[\frac{AEa}{R_g(x)}\right] - 5.331 - 1.052\frac{Ea}{RT} \tag{21}$$

Equation 21 is OFW equation used to determine kinetic parameter of chemical reaction. A plot of $\ln(\beta)$ versus *1/T* gives a straight line, where Ea can be determined from the slope (*slope = -1.052Ea/R*) whereas, A can be determined from the intercept [28, 30].

Model-free methods can be used to study the solid-state kinetics of isothermal and non-isothermal processes. Model-free methods are used to calculate the Ea without assumptions and are commonly used to calculate Ea by grouping, such as A into intercept of linear equation and slope of the equation. Thus, model-free methods only concentrate on activation energy [9]. The Coats-Redfern equation is commonly used to study the kinetics analysis and various kinetics parameters, such as A and Ea [31]. By integrating and rearranging Equation 9, Equation 22 can be obtained:

$$\frac{1-(1-x)^{1-n}}{1-n} = \frac{A}{\beta}\int_0^T e^{-Ea/RT}\, dT \tag{22}$$

By integrating the term $e^{-Ea/RT}$ and neglecting the higher order terms, we got Equation 23:

$$\frac{1-(1-x)^{1-n}}{1-n} = \frac{ART^2}{\beta Ea}\left[1 - \frac{2RT}{Ea} e^{-Ea/RT}\right] \tag{23}$$

Taking the log of Equation 23, Equation 24 can be obtained:

$$\ln\left[\frac{1-(1-x)^{1-n}}{T^2(1-n)}\right] = \ln\left[\frac{AR}{\beta Ea}\left[1-\frac{2RT}{Ea}\right]\right] - \frac{Ea}{RT} \quad (24)$$

The activation energy can be determined by plotting $ln[(1-(1-\alpha)^{1-n}/(1-n)T^2]$ versus $1/T$ [31, 32].

KAS used the integral iso-conversional method for the determination of Ea. In the KAS method, Equation 25 was used to evaluate kinetics parameters [33].

$$\ln\left(\frac{\beta}{T^2}\right) = \ln\left[\frac{AR}{Eag\alpha}\right] - \frac{Ea}{RT} \quad (25)$$

Where $g(\alpha)$ is mathematical function, *T* is the absolute temperature, *Ea* is the activation energy, *A* is an exponential factor, *R* is the gas constant and β is the heating rate. Ea can be calculated from the slope of the curve by plotting $ln\beta/T^2$ versus $1/T$ keeping the *x* constant [34, 35].

FM method is a differential iso-conversional technique that is presented in Equation 26 [36]:

$$\frac{dx}{dt} = \beta\left[\frac{dx}{dt}\right] = Ae^{-Ea/RT}f(x) \quad (26)$$

Taking the natural log for both sides of Equation 26 the following Equation 27 is obtained:

$$\ln\left[\frac{dx}{dt}\right] = \ln\left[\beta\left(\frac{dx}{dt}\right)\right] = \ln[Af(x)] - \frac{Ea}{RT} \quad (27)$$

It is supposed that the conversional factor *f(x)* remains constant, suggesting that the degradation depends only on the rate of mass loss, independent of temperature. Hence activation energy can be calculated from the slope of the line given by the plot of *ln(dx/dt)* versus *1/T* [37, 38].

The thermodynamic parameters such Gibbs free energy, entropy and enthalpy of catalytic pyrolysis of WPS can be calculated using Equations 28 and 29, respectively:

$$\Delta G = E + RT\left[\ln\left(\frac{KT}{hA}\right)\right] \quad (28)$$

$$\Delta S = \frac{\Delta H - \Delta G}{T} \quad (29)$$

Where ΔG is the Gibbs free energy, ΔS is the entropy and ΔH is the enthalpy or heat change in a chemical reaction [39, 40].

3. Results and Discussion

3.1 Thermogravimetric Analysis

To determine the degradation temperature of each component, thermogravimetric analysis of the catalyst, WPS and WPS catalyst mixture (97:3) was carried out at a heating rate of 10°C min^{-1}. Figure 1a showed the TG/DTG results of WPS in the absence and presence of catalyst at 10°C min^{-1}. The results showed that WPS degraded in the temperature range of 350 to 420°C. The nature, composition and structure of the catalyst were not affected during the experiments as all the

decomposition of WPS took place at temperatures below 420°C. The results also indicated that clay catalyst decreased the degradation temperature of WPS. The degradation of pure catalyst is shown in Figure 1b, and the results indicated that natural clay had two-step degradation, with the first step occurring at about 68°C, indicating the loss of water molecules from the clay. The second degradation step took place at 817°C, which was the decomposition of alumina and silica from the clay.

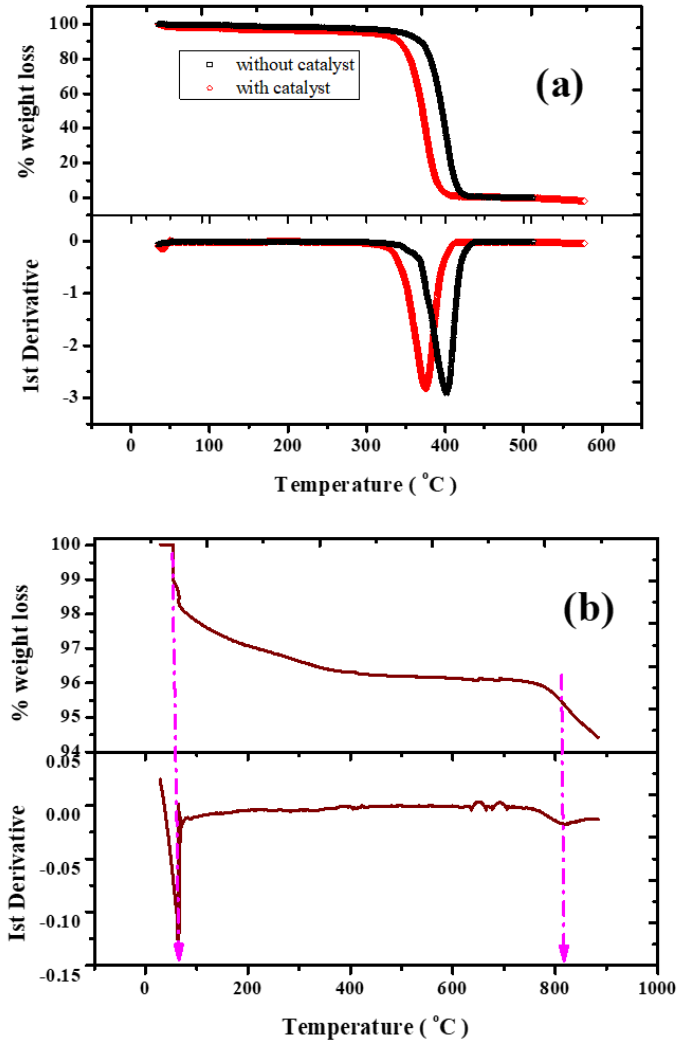

Figure 1 TG/DTG of **(a)** pure and catalytic degradation of WPS and **(b)** TG/DTG of natural clay.

3.2 Kinetic Study

For kinetic analysis, thermogravimetric analysis of WPS with clay as catalyst was performed at 5, 10, 15 and 20°C/min and the obtained data was interpreted using OFW, CR, KAS and FM models to determine the kinetic parameters.

3.2.1 Coats Redfern Model

CR equation was used for the determination of kinetic parameters, where the left-hand side of the equation was plotted against *1000/T* and fraction conversion as shown in Figure 2. Ea and A

were calculated from the slope and intercept of the plots, respectively, as shown in Table 1. The results showed that the correlation coefficient for each straight line was above 0.985. Ea was calculated at various fraction conversions and was found to range from 83.22 to 150.31 kJmol^{-1}. The results in Table 1 indicated that Ea increased with increasing fraction conversion. Where the largest increment of Ea was observed for fraction conversion from 0.7 to 0.8, i.e., 15 kJmol^{-1}. Similarly, A-factor calculated from the intercept ranged from 1.0×10^6 to 5.1×10^{10} min^{-1}. The A-factor value also increased with the increase in fraction conversion, and the average A-factor value was 8.3×10^9 min^{-1}. By comparing our results with the literature, a good agreement was observed. The increase in Ea and A-factor with fraction conversion may be attributed to the complex mechanism of the solid-state reaction.

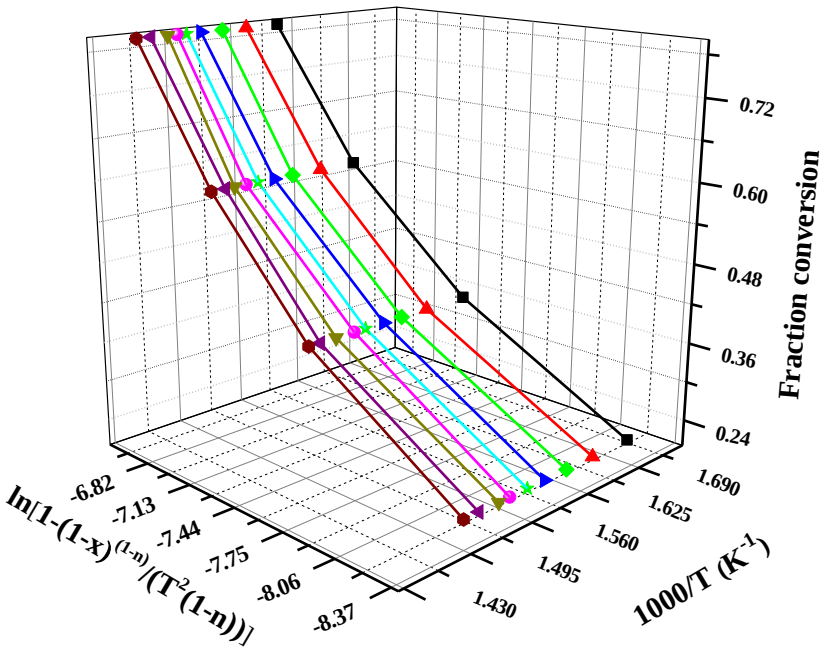

Figure 2 CR plots of various conversions for WPS degradation in the presence of natural clay.

Table 1 Kinetics parameters of WPS calculated using CR method at different degrees of conversion.

α	Ea (kJmol^{-1})	A-factor (min^{-1})	R^2
0.1	83.22	1.0×10^6	0.996
0.2	93.28	4.7×10^6	0.997
0.3	99.10	1.1×10^7	0.991
0.4	104.75	2.7×10^7	0.992
0.5	111.57	7.9×10^7	0.992
0.6	123.37	6.4×10^8	0.985
0.7	129.19	1.6×10^9	0.988
0.8	144.24	2.1×10^{10}	0.999
0.9	150.31	5.1×10^{10}	0.998
Average Ea and A	115.45	8.3×10^9	

According to the literature, the thermal degradation of PS was carried out in an inert atmosphere using nitrogen as an inert gas. Using the Arrhenius equation, Ea was calculated to be 255 kJmol^{-1} in the absence of a catalyst, while in the presence of a catalyst Ea was calculated in the range of 196 to 224 kJmol^{-1}, which is about 40 kJmol^{-1} less compared to the catalytic decomposition [41].

3.2.2 Ozawa-Flynn-Wall Model

OFW, a non-isothermal was used for the determination of the kinetic parameters of WPS. *Lnβ* was plotted against 1000/T and fraction conversion using OFW model and the resultant plots were shown in Figure 3. Where Ea was calculated from the slope and A-factor was determined from the intercept of the plots, and the resultant kinetic parameters determined were listed in Table 2. As the fraction conversion increased from 0.1 to 0.9, the Ea value increased from 74.52 to 133.71 kJmol^{-1}. From the gradual increase in Ea and A-factor, it has been concluded that there is a linear relationship between the conversion degree and kinetic parameters which indicates the existence of progressive bond breakage, i.e., the weaker bonds break first, followed by the stronger ones.

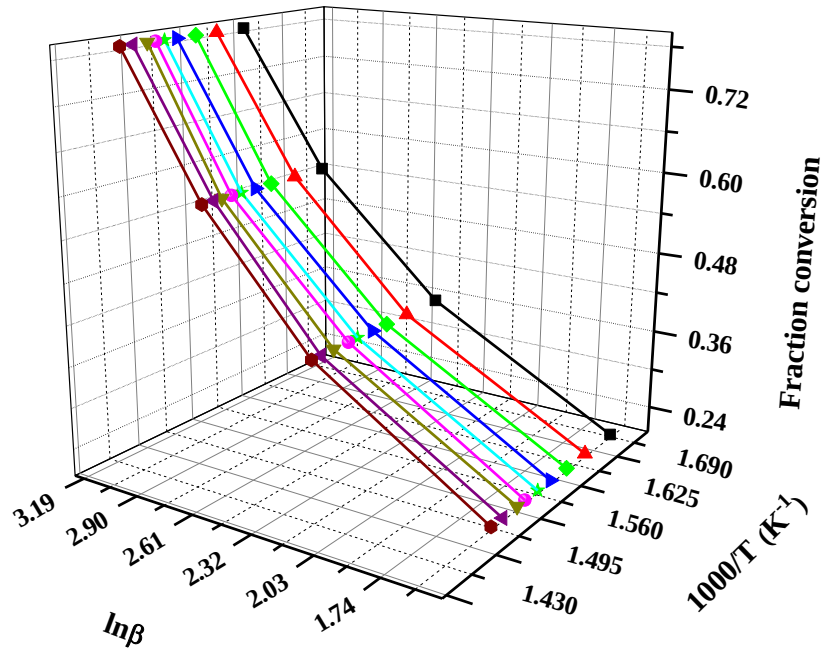

Figure 3 OFW plots at different fraction conversions for WPS decomposition.

Table 2 Ea and A-factor for WPS decomposition obtained from OFW method.

α	Ea (kJmol^{-1})	A-factor (min^{-1})	R^2
0.1	74.52	6.7×10^5	0.995
0.2	83.06	4.7×10^6	0.998
0.3	88.27	1.4×10^7	0.993
0.4	93.25	3.6×10^7	0.991
0.5	99.42	1.1×10^8	0.992
0.6	109.77	8.0×10^8	0.983
0.7	115.22	2.1×10^9	0.993
0.8	128.42	2.1×10^{10}	0.999

0.9	133.71	4.9×10^{10}	0.994
Average Ea and A	102.85	8.2×10^{9}	

Previous studies have investigated the single decomposition of PS by thermogravimetry within the temperature range of 250 to 400°C. The results showed that at the initial stage, a lower Ea was observed, which then increased with fraction conversion. The average activation energy calculated was 200 kJmol^{-1} [19]. In another study, Kwak et al. [42] performed thermal degradation of PS within the temperature range of 370 to 420°C . First-order kinetics and Arrhenius equation were applied for the determination of the rate constant and Ea respectively. The calculated activation energy was 157 kJmol^{-1} in supercritical water and 132 kJmol^{-1} in supercritical n-hexane. These results in the literature are in good agreement with our results in terms of kinetic parameters.

3.2.3 Kissinger-Akahira-Sunose Model

Kinetic parameters were investigated using KAS equation, where $\ln\left(\frac{\beta}{T^2}\right)$ was plotted against 1000/T and fraction conversion, the resultant plots were shown in Figure 4, and the resultant data was presented in Table 3. The results in Table 3 showed correlation coefficients at each fraction conversion ranging from 0.990 to 0.999. Ea determined using KAS equation showed a good linear relationship with fraction conversion, starting from 73.16 kJmol^{-1} and ending with 131.27 kJmol^{-1}. And the Ea investigated using KAS method was the lowest among all models. By comparing kinetic factors, it can be concluded that the variation of both Ea and A-factor with fraction conversions is in good agreement with the relevant literature.

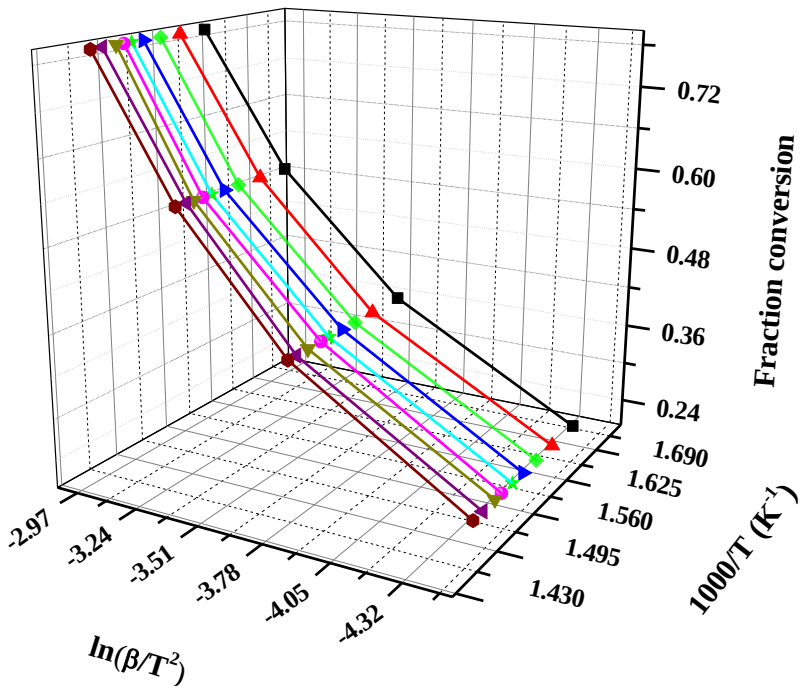

Figure 4 Kinetic plots of WPS using KAS model at various fraction conversions.

Table 3 Ea and A-factor calculated using KAS method for WPS decomposition.

α	Ea (kJmol^{-1})	A-factor (min^{-1})	R^2
0.1	73.16	4.9×10^4	0.994
0.2	81.56	4.2×10^5	0.997
0.3	86.715	1.4×10^6	0.993
0.4	91.53	4.2×10^6	0.990
0.5	97.60	1.5×10^7	0.992
0.6	107.74	1.2×10^8	0.983
0.7	113.15	$3.9 \times x10^8$	0.993
0.8	126.12	4.9×10^9	0.999
0.9	131.27	1.5×10^{10}	0.993
Average Ea and A	100.98	2.2×10^9	

Westerhout et al. [43] performed the pyrolysis of PS below 450°C by thermogravimetry .First-order kinetics was applied for the determination of kinetic parameters, and Ea and A-factor were evaluated using the random chain dissociation method with 204 kJmol^{-1} and 3.3×10^{13} sec^{-1} respectively. Kim et al. [44] investigated the thermal degradation of PS in the presence and absence of the catalyst. The isothermal Ea was calculated using Arrhenius equation and the non-isothermal Ea was calculated using Kissinger equation. It was observed that Ea decreased from 194 to 138 kJmol^{-1} with the use of arcillite as catalyst.

3.2.4 Friedman Model

In the FM model, *Ln(dx/dt)* was plotted against fraction conversion and 1000/T, and the observed straight lines were shown in Figure 5. Ea and A-factor determined by the FM method are given in Table 4. Ea calculated using the FM model ranged from 78.40 to 140.67 kJmol^{-1}, which was higher than that calculated by other models. However, the FM method showed a linear correlation of Ea with fraction conversion. The average Ea for WPS using natural clay catalyst was 108.90 kJmol^{-1}, this activation is still lower than reported in the literature. Similarly, A-factor investigated by the FM model was also in linear relation with conversion. The average A-factor calculated from the FM method was 2.4×10^{10} min^{-1}. When compared to fraction conversion, all the kinetic parameters showed a linear increment, indicating that the breakage of linkage is gradual, with weaker bonds broken first followed by complex ones. Those stronger bonds need more energy for breakage, hence higher Ea was observed.

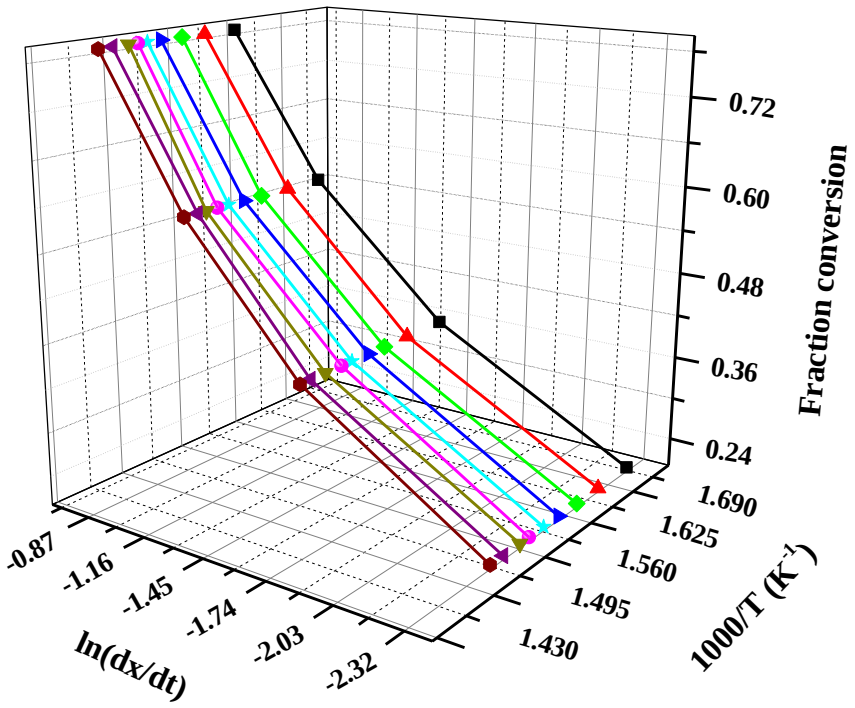

Figure 5 FM plots of WPS decomposition at different fraction conversions for determining kinetic parameters.

Table 4 Kinetics parameters determined at different degrees of conversion for WPS using the FM method.

α	Ea (kJmol^{-1})	A-factor (min^{-1})	R^2
0.1	78.40	1.3×10^6	0.995
0.2	87.38	5.9×10^6	0.998
0.3	92.86	1.4×10^7	0.993
0.4	98.10	3.4×10^7	0.991
0.5	104.59	1.1×10^8	0.992
0.6	115.48	8.9×10^8	0.983
0.7	121.21	2.8×10^9	0.993
0.8	135.10	4.1×10^{10}	0.999
0.9	140.67	1.7×10^{11}	0.994
Average Ea and A	108.20	2.4×10^{10}	

Marcilla and Beltran [45] carried out thermal degradation of PS at different heating rates and first-order kinetics were applied for the determination of kinetic parameters. All the experiments were carried out in an inert atmosphere using nitrogen gas. The results indicated that Ea and A-factor ranged from 186 to 276 kJmol^{-1} and 8.5×10^{13} to 3.6×10^{19} min^{-1} respectively.

3.3 Comparison of Activation Energies

Figure 6 showed that the Ea increased linearly with the fraction conversion. The initial low Ea showed the cleavage of weak bonds and the elimination of volatile compounds. However, the

cleavage of strong bonds required high temperatures, so the cleavage of stable compounds required greater Ea. It can be also seen in Figure 6 that the Ea calculated by the CR model is greater than that calculated by other models, while the Ea calculated by the KAS method is the lowest of all models. However, the apparent Ea determined by these models are in good agreement with each other and the literature.

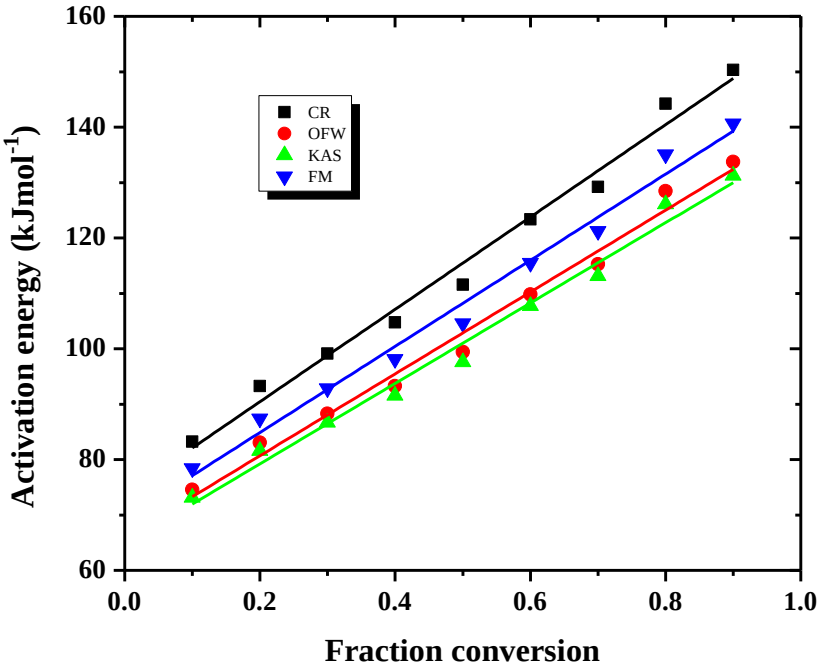

Figure 6 Variation of Ea obtained from different models with fraction conversion for WPS decomposition.

Chrissafis [46] established a relationship between Ea and fraction conversion, obtaining a constant average value. A small difference in Ea was observed, which was due to systematic error. A constant Ea was calculated by the OFW method. In another study, a relationship between Ea and fraction conversion was investigated using different models. It was found that there was a close agreement between Ea from OFW and KAS models. Al-Bayaty and Farhan [47] determined Ea for the decomposition of PS at different heating rates and observed a slight variation in Ea with fraction conversion.

3.4 Order of Reaction

The order of reaction was determined using the CR model. Various orders (n = 0, 1, 2, 3) were applied to the CR model and the result are shown in Figure 7. The results indicated that the highest correlation coefficient value was observed for n = 1, suggesting that thermal degradation of WPS follows first-order kinetics. Thermocatalytic degradation of WPS and polyethylene were carried out by Miskolczi et al. [41]. The effect of catalyst on WPS degradation was investigated through non-isothermal studies and kinetic study was carried out by applying the Arrhenius equation. It was found that the order of reaction of WPS thermocatalytic decomposition was first order. Similarly, several researchers used different kinetic models to investigate the order of reaction for thermal

and catalytic pyrolysis of waste polymers and concluded that degradation of WPS follows first-order reaction, which is in good agreement with our results [48-50].

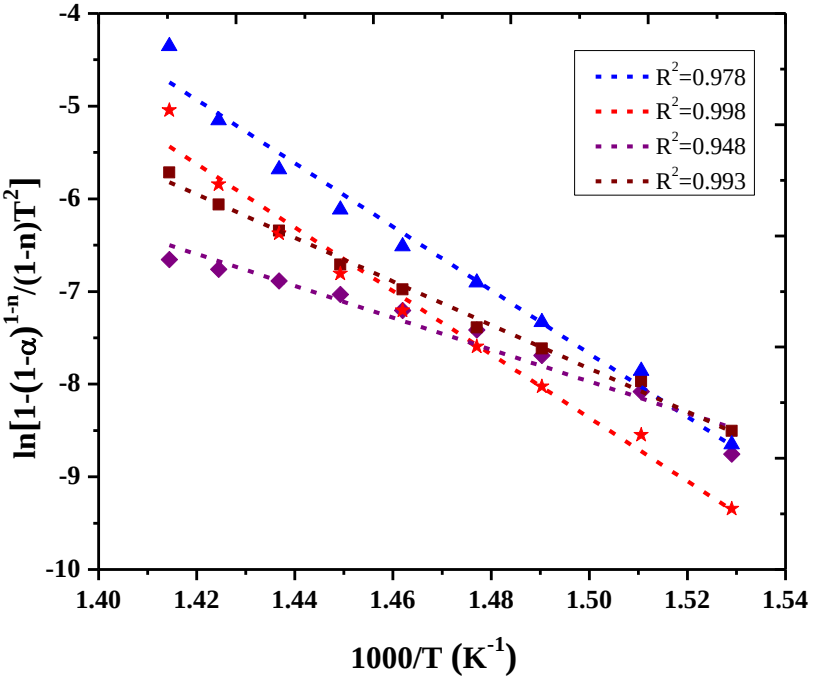

Figure 7 Plots for determination of reaction order for WPS degradation using CR method.

3.5 Comparison with the Literature

As shown in Table 5, Ea and A-factor determined by CR, OFW, KAS and FM models in previous literature were compared with those determined in this study. The table showed that the Ea determined by all four methods were quite reasonable. It can be seen that the Ea and A-factor determined in our research work are in good agreement with the values previously reported in the literature. In our work, the consistency and low values of Ea are due to the use of a suitable natural catalyst.

Table 5 Comparison of kinetics parameters of WPS with those described in the literature.

T (°C)	Atmos:	Ea (kJmol^{-1})	A-factor (min^{-1})	Model used	References
200-600	Vacuum	165-176	6.1×10^{12}-3.6×10^{13}	Risby and Yergey	[51]
100-600	Vacuum	177	3.5×10^{11}	Arrhenius	[52]
400-450	Nitrogen	219	1.3×10^{14}	1st Order K. Model	[43]
30-600	Nitrogen	200	---	Modified Arrhenius	[19]
200-550	Nitrogen	312	1.31×10^{9}	Parallel reac; model	[53]
100-900	Nitrogen	251.9	5.2×10^{14}	CR	[54]
100-900	Nitrogen	261.4	1.5×10^{15}	Freeman-Carol	[54]
100-900	Nitrogen	260.1	1.2×10^{15}	Reich-Levi	[54]
375-425	Nitrogen	138-194	---	K	[44]
282-398	Nitrogen	199	7.1×10^{15}	CR, Achar	[55]

380-420	Nitrogen	94.7-211.4	2.6×10^{4}-3.1×10^{14}	Arrhenius	[56]
200-280	Nitrogen	151-161	24.6-29.2	MacCllum Model	[57]
200-280	Nitrogen	161	31	Wilkinson Model	[57]
200-280	Nitrogen	152	29	Arrhenius	[57]
200-280	Nitrogen	149	24.6	K	[57]
400	Vacuum	360	----	OFW	[16]
50-600	Nitrogen	179-200	7.2×10^{10}-3.9×10^{12}	OFW	[14]
40-800	Nitrogen	122-242	1.8×10^{14}-2.65×10^{18}	FM	[58]
40-800	Nitrogen	126-239	1.8×10^{14}-2.65×10^{18}	KAS	[58]
40-800	Nitrogen	188-206	1.8×10^{14}-2.65×10^{18}	CR	[58]
50-600	Nitrogen	179-200	7.2×10^{10}-3.9×10^{12}	OFW	[14]
40-600	Nitrogen	83-150	1.0×10^{6}-5.1×10^{10}	CR	Present work
40-600	Nitrogen	74-133	6.7×10^{5}-4.9×10^{10}	OFW	Present work
40-600	Nitrogen	73-131	4.9×10^{4}-1.5×10^{10}	KAS	Present work
40-600	Nitrogen	78-140	1.3×10^{6}-1.7×10^{11}	FM	Present work

3.6 Thermodynamic Study

Thermodynamic parameters were used to investigate whether the reaction was spontaneous or non-spontaneous. Thermodynamic study of WPS was carried out at various temperatures and the resultant plots are shown in Figure 8. The results indicated a linear relation of fraction conversion with the inverse of temperature and *ln(K/T).* Slope and intercept were used to investigate thermodynamic parameters i.e., entropy, enthalpy and Gibbs free energy are shown in Table 6. The enthalpy at the beginning of the conversion was 73.16 $kJmol^{-1}$and grew to 134.68 $kJmol^{-1}$ at the end of the conversion, indicating a linear increase in enthalpy with fraction conversion. Similarly, the entropy of the decomposition reaction ranged from -134.97 to -77.55 $Jmol^{-1}K^{-1}$ and Gibbs free energy ranged from 195.71 to 210.05 $kJmol^{-1}$. Gibbs free energy showed linear relation with fraction conversion, indicating larger molecules have greater free energy compared to low molecular weight molecules. Chen et al., [59] investigated the decomposition of waste material under non-isothermal conditions. Thermogravimetric analysis was carried out at different heating rates the resultant data was interpreted for kinetics and thermodynamics. Thermodynamic parameters such as Gibbs free energy, enthalpy and entropy ranged from 151.18 to 189.6, 90.94 to 95.31 $kJmol^{-1}$ and -131.4 to -147.5 $Jmol^{-1}K^{-1}$ respectively. Similarly, several other studies have reported thermodynamic parameters of various waste materials that are in good agreement with our results [60-62].

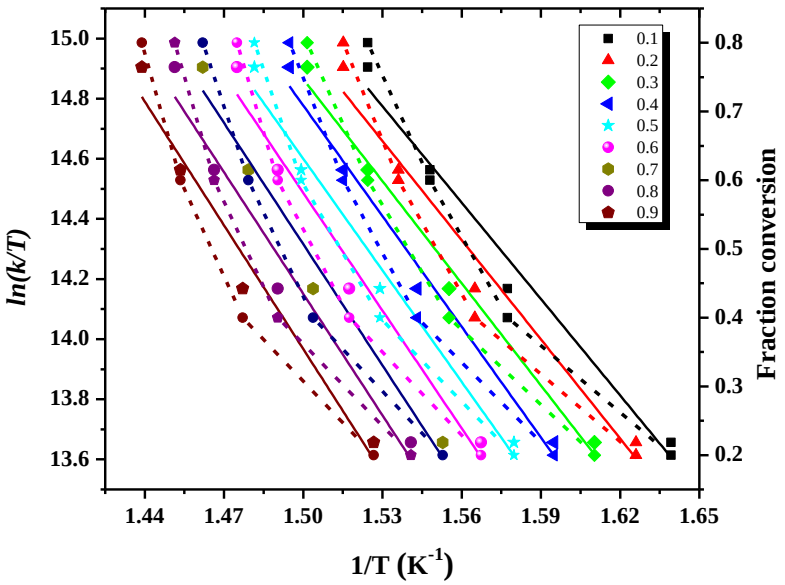

Figure 8 Plots of WPS decomposition for determination of thermodynamic parameters.

Table 6 Thermodynamic parameters of thermocatalytic degradation of WPS at various fractions of conversion.

S.No	Fraction conversion	ΔH kJmol^{-1}	−ΔS Jmol^{-1}K^{-1}	ΔG kJmol^{-1}
1	0.1	73.16	134.97	195.71
2	0.2	81.47	126.88	197.95
3	0.3	86.46	122.34	199.74
4	0.4	92.53	117.05	202.20
5	0.5	109.07	100.58	204.22
6	0.6	113.15	97.22	205.79
7	0.7	126.95	83.48	206.91
8	0.8	132.94	78.14	208.26
9	0.9	134.68	77.55	210.05

4. Conclusion

In the present work, catalytic degradation of WPS was carried out under non-isothermal conditions. Thermogravimetric analysis was performed at different heating rates (5, 10, 15 and 20°C min^{-1}) within the temperature range of 40 to 600°C. Kinetic parameters were determined at different fraction conversions using CR, OFW, KAS and FM models and were found to range from 83-150, 74-133, 73-131 and 78-140 kJmol^{-1} respectively. Similarly, the A-factor range was determined as 1.0×10^{6}-5.1×10^{10}, 6.7×10^{5}-4.9×10^{10}, 4.9×10^{4}-1.5×10^{10} and 1.3×10^{6}-1.7×10^{11} min^{-1} respectively. The values of Ea and A-factor calculated by KAS were consistent and lowest. However, the kinetic parameters investigated by all four models are in good agreement with each other and the reported literature. Hence, it has been concluded that natural clay catalyst shows great efficiency by decreasing the Ea. The kinetic parameters are very helpful in determining the reaction mechanism of solid-state reactions in industrial systems.

Acknowledgments

Higher Education Commission of Pakistan is highly acknowledged.

Author Contributions

Dr. Ghulam Ali: Investigation, Visualization, Conceptualization, Methodology, Writing original draft, Writing – review & editing, Results and analysis. **Dr. Jan Nisar:** Conceptualization, Funding acquisition, Supervision, Project administration.

Competing Interests

It is declared that the authors have no conflicts of interest that could have appeared to influence the work reported in this paper.

References

1. Levine SE, Broadbelt LJ. Reaction pathways to dimer in polystyrene pyrolysis: A mechanistic modeling study. Polym Degrad Stab. 2008; 93: 941-951.
2. Municipal solid waste in the United States: 2000 facts and figures. Washington: US EPA; 2002.
3. Municipal solid waste in the. United States: 2005 facts and figures. Washington: US EPA; 2006.
4. Karagöz S, Karayildirim T, Uçar S, Yuksel M, Yanik J. Liquefaction of municipal waste plastics in VGO over acidic and non-acidic catalysts. Fuel. 2003; 82: 415-423.
5. Ali G, Nisar J, Shah A, Farooqi ZH, Iqbal M, Shah MR, et al. Production of liquid fuel from polystyrene waste: Process optimization and characterization of pyrolyzates. Combust Sci Technol. 2021: 1-14. doi: 0.1080/00102202.2021.1985481.
6. Kiran N, Ekinci E, Snape CE. Recyling of plastic wastes via pyrolysis. Resour Conserv Recycl. 2000; 29: 273-283.
7. Poutsma ML. Mechanistic analysis and thermochemical kinetic simulation of the pathways for volatile product formation from pyrolysis of polystyrene, especially for the dimer. Polym Degrad Stab. 2006; 91: 2979-3009.
8. Li N, Cho AS, Broadbelt LJ, Hutchinson RA. Low conversion 4-acetoxystyrene free-radical polymerization kinetics determined by pulsed-laser and thermal polymerization. Macromol Chem Phys. 2006; 207: 1429-1438.
9. Khawam A. Application of solid-state kinetics to desolvation reactions. Iowa City: The University of Iowa; 2007.
10. Khawam A, Flanagan DR. Complementary use of model-free and modelistic methods in the analysis of solid-state kinetics. J Phys Chem B. 2005; 109: 10073-10080.
11. Opfermann JR, Kaisersberger E, Flammersheim HJ. Model-free analysis of thermoanalytical data-advantages and limitations. Thermochim Acta. 2002; 391: 119-127.
12. Amjad UeS, Ishaq M, Rehman Hu, Ahmad N, Sherin L, Hussain M, et al. Diesel and gasoline like fuel production with minimum styrene content from catalytic pyrolysis of polystyrene. Environm Prog Sustain Energy. 2021; 40: e13493.
13. Joshi CA, Seay JR. Total generation and combustion emissions of plastic derived fuels: A trash to tank approach. Environ Prog Sustain Energy. 2020; 39. doi: 10.1002/ep.13151.

14. Şenocak A, Alkan C, Karadağ A. Thermal decomposition and a kinetic study of poly(para-substituted styrene)s. Am J Analyt Chem. 2016; 7: 246-253.
15. Aboulkas A, El harfi K, Nadifiyine M, El bouadili A. Investigation on pyrolysis of Moroccan oil shale/plastic mixtures by thermogravimetric analysis. Fuel Process Technol. 2008; 89: 1000-1006.
16. Singh KKK, Singh SP. Kinetic model & analysis for pyrolysis of waste polystyrene over laumontite. Int J Eng Res. 2013; 2. doi: 10.17577/IJERTV2IS2427.
17. Oh SC, Han DI, Kwak H, Bae SY, Lee KH. Kinetics of the degradation of polystyrene in supercritical acetone. Polym Degrad Stab. 2007; 92: 1622-1625.
18. Kyaw KT, Hmwe CSS. Effect of various catalysts on fuel oil pyrolysis process of mixed plastic wastes. Int J Adv Eng Technol. 2015; 8: 794.
19. Peterson JD, Vyazovkin S, Wight CA. Kinetics of the thermal and thermo-oxidative degradation of polystyrene, polyethylene and poly(propylene). Macromol Chem Phys. 2001; 202: 775-784.
20. Vyazovkin S, Burnham AK, Criado JM, Pérez-Maqueda LA, Popescu C, Sbirrazzuoli N. ICTAC kinetics committee recommendations for performing kinetic computations on thermal analysis data. Thermochim Acta. 2011; 520: 1-19.
21. Vyazovkin S, Chrissafis K, Di Lorenzo ML, Koga N, Pijolat M, Roduit B, et al. ICTAC kinetics committee recommendations for collecting experimental thermal analysis data for kinetic computations. Thermochim Acta. 2014; 590: 1-23.
22. Xia L, Zuo L, Wang X, Lu D, Guan R. Non-isothermal kinetics of thermal degradation of DGEBA/TU-DETA epoxy system. J Adhes Sci Technol. 2014; 28: 1792-1807.
23. Vyazovkin S. Kinetic concepts of thermally stimulated reactions in solids: A view from a historical perspective. Int Rev Phys Chem. 2000; 19: 45-60.
24. Ali G, Nisar J, Iqbal M, Shah A, Abbas M, Shah MR, et al. Thermo-catalytic decomposition of polystyrene waste: Comparative analysis using different kinetic models. Waste Manag Res. 2020; 38: 202-212.
25. Doyle CD. Kinetic analysis of thermogravimetric data. J Appl Polym Sci. 1961; 5: 285-292.
26. Flynn JH, Wall LA. General treatment of the thermogravimetry of polymers. J Res Natl Bur Stand A Phys Chem. 1966; 70A: 487-523.
27. Tiptipakorn S, Damrongsakkul S, Ando S, Hemvichian K, Rimdusit S. Thermal degradation behaviors of polybenzoxazine and silicon-containing polyimide blends. Polym Degrad Stab. 2007; 92: 1265-1278.
28. Ozawa T. A new method of analyzing thermogravimetric data. Bull Chem Soc Jpn. 1965; 38: 1881-1886.
29. Sbirrazzuoli N, Girault Y, Elégant L. Simulations for evaluation of kinetic methods in differential scanning calorimetry. Part 3 — Peak maximum evolution methods and isoconversional methods. Thermochim Acta. 1997; 293: 25-37.
30. Flynn JH, Wall LA. A quick, direct method for the determination of activation energy from thermogravimetric data. J Polym Sci Part B Polym Lett. 1966; 4: 323-328.
31. Coats AW, Redfern JP. Kinetic parameters from thermogravimetric data. Nature. 1964; 201: 68-69.
32. Zhou L, Luo T, Huang Q. Co-pyrolysis characteristics and kinetics of coal and plastic blends. Energy Convers Manag. 2009; 50: 705-710.

33. Nisar J, Ali G, Shah A, Farooqi ZH, Iqbal M, Khan S, et al. Production of fuel oil and combustible gases from pyrolysis of polystyrene waste: Kinetics and thermodynamics interpretation. Environ Technol Innov. 2021; 24: 101996.
34. Kissinger HE. Variation of peak temperature with heating rate in differential thermal analysis. J Res Natl Bur Stand. 1956; 57: 217-221.
35. Kissinger HE. Reaction kinetics in differential thermal analysis. Analyt Chem. 1957; 29: 1702-1706.
36. Nisar J, Ali G, Shah A, Shah MR, Iqbal M, Ashiq MN, et al. Pyrolysis of expanded waste polystyrene: Influence of nickel-doped copper oxide on kinetics, thermodynamics, and product distribution. Energy Fuels. 2019; 33: 12666-12678.
37. Friedman HL. Kinetics of thermal degradation of char-forming plastics from thermogravimetry. Application to a phenolic plastic. J Polym Sci Part C Polym Symp. 1964; 6: 183-195.
38. Friedman HL. New methods for evaluating kinetic parameters from thermal analysis data. J Polym Sci Part B Polym Lett. 1969; 7: 41-46.
39. Yuan X, He T, Cao H, Yuan Q. Cattle manure pyrolysis process: Kinetic and thermodynamic analysis with isoconversional methods. Renew Energy. 2017; 107: 489-496.
40. Xu Y, Chen B. Investigation of thermodynamic parameters in the pyrolysis conversion of biomass and manure to biochars using thermogravimetric analysis. Bioresour Technol. 2013; 146: 485-493.
41. Miskolczi N, Bartha L, Deák G. Thermal degradation of polyethylene and polystyrene from the packaging industry over different catalysts into fuel-like feed stocks. Polym Degrad Stab. 2006; 91: 517-526.
42. Kwak H, Shin HY, Bae SY, Kumazawa H. Characteristics and kinetics of degradation of polystyrene in supercritical water. J Appl Polym Sci. 2006; 101: 695-700.
43. Westerhout RWJ, Waanders J, Kuipers JAM, van Swaaij WPM. Kinetics of the low-temperature pyrolysis of polyethene, polypropene, and polystyrene modeling, experimental determination, and comparison with literature models and data. Ind Eng Chem Res. 1997; 36: 1955-1964.
44. Kim JS, Lee WY, Lee SB, Kim SB, Choi MJ. Degradation of polystyrene waste over base promoted fe catalysts. Catal Today. 2003; 87: 59-68.
45. Marcilla A, Beltran M. Kinetic study of the thermal decomposition of polystyrene and polyethylene-vinyl acetate graft copolymers by thermogravimetric analysis. Polym Degrad Stab. 1995; 50: 117-124.
46. Chrissafis K. Kinetics of thermal degradation of polymers. J Therm Anal Calorim. 2009; 95: 273-283.
47. Al-Bayaty SA, Farhan AJ. Thermal decomposition kinetics unsaturated polyester and unsaturated polyester reinforcement by toner carbon nano powder (TCNP) composites. Int J Appl Innov Eng Manag. 2015; 4: 139-146.
48. Lee SY, Yoon JH, Kim JR, Park DW. Catalytic degradation of polystyrene over natural clinoptilolite zeolite. Polym Degrad Stab. 2001; 74: 297-305.
49. Jun HC, Oh SC, Lee HP, Kim HT. A kinetic analysis of the thermal-oxidative decomposition of expandable polystyrene. Korean J Chem Eng. 2006; 23: 761-766.
50. Lee KH, Noh NS, Shin DH, Seo Y. Comparison of plastic types for catalytic degradation of waste plastics into liquid product with spent FCC catalyst. Polym Degrad Stab. 2002; 78: 539-544.

51. Risby TH, Yergey JA, Scocca JJ. Linear programmed thermal degradation mass spectrometry of polystyrene and poly(vinyl chloride). Analyt Chem. 1982; 54: 2228-2233.
52. Sato A, Kaneko K. Differential thermal and chromatographic analysis on pyrolysis of plastics. J Energy Heat Mass Transfer. 1983; 5: 323-338.
53. Sørum L, Grønli MG, Hustad JE. Pyrolysis characteristics and kinetics of municipal solid wastes. Fuel. 2001; 80: 1217-1227.
54. Lisa G, Avram E, Paduraru G, Irimia M, Hurduc N, Aelenei N. Thermal behaviour of polystyrene, polysulfone and their substituted derivatives. Polym Degrad Stab. 2003; 82: 73-79.
55. Zeng W, Chow WK, Yao B. Chemical kinetics and mechanism of polystyrene thermal decomposition. Proceedings of 7th Asia-Oceania Symposium on Fire Science & Technology; 2007 September 20-22; Hong Kong, China. International Association for Fire Safety Science.
56. Costa P, Pinto F, Ramos A, Gulyurtlu I, Cabrita I, Bernardo M. Study of the pyrolysis kinetics of a mixture of polyethylene, polypropylene, and polystyrene. Energy Fuels. 2010; 24: 6239-6247.
57. Blanco I, Abate L, Antonelli ML. The regression of isothermal thermogravimetric data to evaluate degradation E_a values of polymers: A comparison with literature methods and an evaluation of lifetime prediction reliability. Polym Degrad Stab. 2011; 96: 1947-1954.
58. Cheng J, Pan Y, Yao J, Wang X, Pan F, Jiang J. Mechanisms and kinetics studies on the thermal decomposition of micron poly (methyl methacrylate) and polystyrene. J Loss Prevent Process Ind. 2016; 40: 139-146.
59. Chen J, Wang Y, Lang X, Ren Xe, Fan S. Evaluation of agricultural residues pyrolysis under non-isothermal conditions: Thermal behaviors, kinetics, and thermodynamics. Bioresour Technol. 2017; 241: 340-348.
60. Boonchom B, Puttawong S. Thermodynamics and kinetics of the dehydration reaction of $FePO_4{\cdot}2H_2O$. Physica B Condens Matter. 2010; 405: 2350-2355.
61. Chen Fx, Zhou Cr, Li Gp, Peng Ff. Thermodynamics and kinetics of glyphosate adsorption on resin D301. Arab J Chem. 2016; 9: S1665-S1669.
62. Li X, Zhou X, Mu J, Lu L, Han D, Lu C, et al. Thermodynamics and kinetics of p-aminophenol adsorption on poly(aryl ether ketone) containing pendant carboxyl groups. J Chem Eng Data. 2011; 56: 4274-4277.